Chemically Tuning Attractive and Repulsive Interactions between Solubilizing Oil Droplets

Ciera M. Wentworth[1], Alexander C. Castonguay[1], Pepijn G. Moerman[2], Caleb H. Meredith[3], Rebecca V. Balaj[1], Seong Ik Cheon[1], and Lauren D. Zarzar*[1,3,4]

1. C. Wentworth, A. C. Castonguay, Dr. R. V. Balaj, Dr. S. Cheon, Dr. L. D. Zarzar
   Department of Chemistry
   The Pennsylvania State University, University Park, PA 16802, USA
   Ldz4@psu.edu
2. Dr. P. G. Moerman
   Department of Chemical and Biomolecular Engineering
   Johns Hopkins University, Baltimore, MD 21218, USA
3. Dr. C. H. Meredith, Dr. L. D. Zarzar
   Department of Materials Science and Engineering
   The Pennsylvania State University, University Park, PA 16802, USA
4. Dr. L. D. Zarzar
   Materials Research Institute
   The Pennsylvania State University, University Park, PA 16802, USA

Abstract. Micellar solubilization is a transport process occurring in surfactant-stabilized emulsions that can lead to Marangoni flow and droplet motility. Active droplets exhibit self-propulsion and pairwise repulsion due to solubilization processes and/or solubilization products raising the droplet's interfacial tension. Here, we report emulsions with the opposite behavior, wherein solubilization decreases the interfacial tension and causes droplets to attract. We characterize the influence of oil chemical structure, nonionic surfactant structure, and surfactant concentration on the interfacial tensions and Marangoni flows of solubilizing oil-in-water drops. Three regimes corresponding to droplet "attraction", "repulsion" or "inactivity" are identified. We believe these studies contribute to a fundamental understanding of solubilization processes in emulsions and provide guidance as to how chemical parameters can influence the dynamics and chemotactic interactions between active droplets.

Introduction

Surfactant-stabilized emulsions have emerged as versatile materials within which to study and design chemotactic colloidal motion, interactions, and collective behavior[1]. A mechanism commonly exploited to drive droplet chemotaxis is the Marangoni effect, wherein interfacial tension gradients along the droplet surface lead to convective flows and droplet motion[2]. Interfacial tension gradients can arise due to mechanisms such as: reactions that produce or degrade interfacially active molecules[3], externally applied fields[4], or by the transfer of droplet contents into the continuous surfactant micellar phase via the process of micellar solubilization[2, 5]. Even spherical, isotropic droplets can be self-propelled via micellar solubilization when advective transport dominates over diffusion (i.e. high Péclet number), leading to a feedback process that sustains a local solubilizate gradient, and hence interfacial tension gradient, across the drop surface[1e, 2, 6]. Solubilizing, motile droplets of many compositions have been demonstrated, including water-in-oil[2] and oil-in-water[5, 7] droplets, multiphase droplets[8], and

droplets stabilized by both ionic[7, 9] and nonionic[10] surfactants. The chemical gradients of solubilizate produced by the micellar solubilization process can also lead to longer-range chemotactic interactions between droplets such as pairwise repulsion[11], chasing[12], and multi-drop collective dynamics[12-13].

It has been proposed that solubilizate "fills" or "swells" micelles, effectively removing surfactant monomer from the vicinity of the drop interface which raises interfacial tension[1a, 14]. Hence, motile solubilizing droplets move from high to low solubilizate concentration. For example, self-propelled oil-in-water droplets move from areas containing "oil-filled" micelles towards regions of "empty" micelles. The observation that interfacial tension is raised by solubilization and/or the products of solubilization is not intuitive[15]. Experiments are conducted at surfactant concentrations orders of magnitude higher than the critical micelle concentration (CMC), above which interfacial tension is not typically expected to change. Possible explanations include that the presence of solubilizate lowers the CMC[7] or that the aggregation number of surfactants in the micelle increases when solubilizate is introduced[14]. It is not clear why solubilization would raise the interfacial tension, rather than lower it, and in what cases a change in interfacial tension would be expected to occur at all. Understanding how solubilization affects interfacial tension would facilitate the tuning of the chemotactic droplet behaviors as well as provide a deeper fundamental understanding of interfacial phenomena in emulsions.

Here, we report a systematic investigation of how oil chemical structure, nonionic surfactant structure, and surfactant concentration collectively influence the effects of oil solubilization on the interfacial tensions, flow profiles, and interactions between oil-in-water droplets. We focus on the interfacial properties of haloalkane oil drops with carbon numbers between 5 and 16 in nonionic surfactants of varying headgroup size at concentrations (1 to 5 wt%) that are above the CMC. We identify regimes in which droplets are "repulsive", "inactive", but also "attractive". Droplets with "repulsive" Marangoni flows exhibit the expected behavior for solubilizing active drops, e.g. solubilized oil raises interfacial tension. However, droplets with "attractive" flow exhibit the opposite behavior: solubilized oil decreases interfacial tension, and isolated drops advect fluid from the bottom of the drop to the top. Within the bounds of conditions tested, we find that attractive flow is favored for lower carbon number oils, surfactants with higher EO numbers in the headgroup, and lower surfactant concentrations. Droplets that are "inactive", i.e. have no discernable Marangoni flow, can in many cases still be solubilizing at an appreciable rate; surprisingly, we find conditions of inactivity falling between attractive and repulsive regimes. By doping the surfactant solution with oil pre-filled into micelles, Marangoni flows can be induced within otherwise inactive droplets by reverse oil transport from micelles into the droplet. We believe these systematic investigations provide insight into how the balance of different chemical factors collectively influence micellar solubilization and oil-water interfacial tensions and discuss plausible mechanisms. Our results suggest that there exists a rich diversity of chemotactic droplet behaviors accessible that can be harnessed for design of liquid active matter.

Results and Discussion

Our first observations regarding differences between repulsive and attractive droplet interactions were made when using bromo-*n*-alkane oil droplets of varying carbon number (bromopentane, bromohexane, and bromooctane) stabilized with nonionic nonylphenylethoxylate surfactant, Tergitol NP-12 (hereafter "NP-12", CMC=0.0085 wt%).

Bromoalkane droplets sink in aqueous solution lending to ease of experimentation and have been shown previously to exhibit solubilization-driven active behavior[10, 12]. To prepare polydisperse droplets (~10 to 200 µm diameter), we emulsified 50 µL of each bromoalkane in 300 µL of aqueous NP-12 of varying concentration via vortex mixing. We transferred approximately 40 droplets to a 1.5" diameter glass-bottom, open top dish containing 1 mL of the same surfactant and viewed the drops under a brightfield optical transmission microscope. Bromohexane droplets in 5 wt% NP-12 repelled one another and spread out across the substrate (**Figure 1A-i**). The solubilization rate, defined as the change in drop diameter over time (-dD/dt) averaged from three isolated droplets, was 13.9 ± 0.7 µm/min. (Refer to SI Section "Solubilization rate measurements" for details. Note that a positive value of solubilization rate corresponds to a droplet shrinking in diameter and that the solubilization rate is independent of starting drop diameter for the drop sizes used). In 1 wt% NP-12, the bromohexane droplets exhibited qualitatively different behavior: droplets attracted each other over 1-2 body lengths and formed clusters (**Figure 1A-ii**) with -dD/dt = 0.8 ± 0.1 µm/min. We next compared droplets of two different oils, bromooctane and bromopentane, but at the same NP-12 concentration (2 wt%). Bromooctane droplets repelled one another (**Figure 1B-i**) with -dD/dt = 3.2 ± 0.2 µm/min, while in contrast, bromopentane droplets attracted each other (**Figure 1B-ii**) with -dD/dt = 1.8 ± 0.7 µm/min.

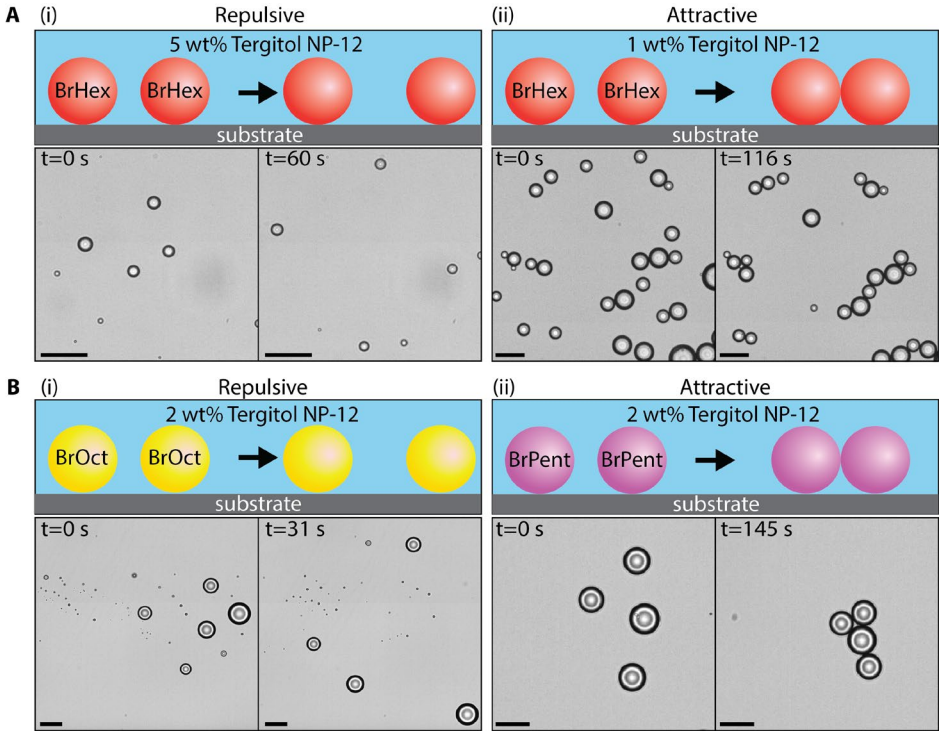

Figure 1: Solubilizing droplets can be repulsive or attractive depending on oil composition and surfactant concentration. **A,** Time lapse optical micrographs with schematics showing that bromohexane (BrHex) droplets are **(A-i)** repulsive in 5 wt% Tergitol NP-12 and **(A-ii)** attractive in 1 wt%. **B,** Time lapse optical micrographs with schematics showing **(B-i)** repulsion between bromooctane (BrOct) droplets and **(B-ii)** attraction between bromopentane (BrPent) droplets in 2 wt% Tergitol NP-12. Scale, 50 µm.

To gain insight as to why some droplets were attractive and some repulsive, we aimed to visualize the Marangoni flows surrounding isolated, solubilizing droplets and quantify differences in interfacial tension along the droplet surface. We first examined bromooctane and bromopentane droplets in 2 wt% NP-12 because they had similar solubilization rates (given above) yet exhibited repulsive or attractive behavior, respectively. A single, isolated ~100 µm diameter bromooctane droplet was extracted from a freshly prepared polydisperse emulsion and added to a glass 0.5 cm x 1 cm cuvette containing 400 µL of 2 wt% NP-12. 1 µm polystyrene tracer particles were suspended in the aqueous phase to aid in flow visualization. Videos of the particle flow around the profile of the droplet were collected using a microscope with the objective lens oriented parallel to the cuvette bottom (**Figure S1, Video S1, S2**). Images were analyzed with particle image velocimetry (PIV) (**Figure 2A**) to extract flow speed and direction. (Refer to SI section, "Particle tracking for flow maps and speed measurements"). As seen in the PIV traces in **Figure 2A**, the repulsive bromooctane droplet pumped fluid from top to bottom and outwards along the substrate away from the droplet, and the droplet levitated above the surface (**Figure 2A-i**). The same experiment was then repeated with an isolated bromopentane droplet in 2 wt% NP-12 (**Figure 2A-ii**). The attractive bromopentane exhibited flows that were qualitatively different, where solution was advected from the bottom of the droplet to the top, and a vortex formed near the substrate (**Figure 2A-ii**). We henceforth call these two different flow types "repulsive flow" and "attractive flow", respectively. To determine whether the surface chemistry of the substrate played a role, we tested the same systems using glass substrates that were functionalized with *N*-(triethoxysilylpropyl)-o-polyethylene oxide urethane (hydrophilic) or hexadecyltrimethoxysilane (hydrophobic). No effect was observed, so further measurements were therefore conducted with untreated glass substrates.

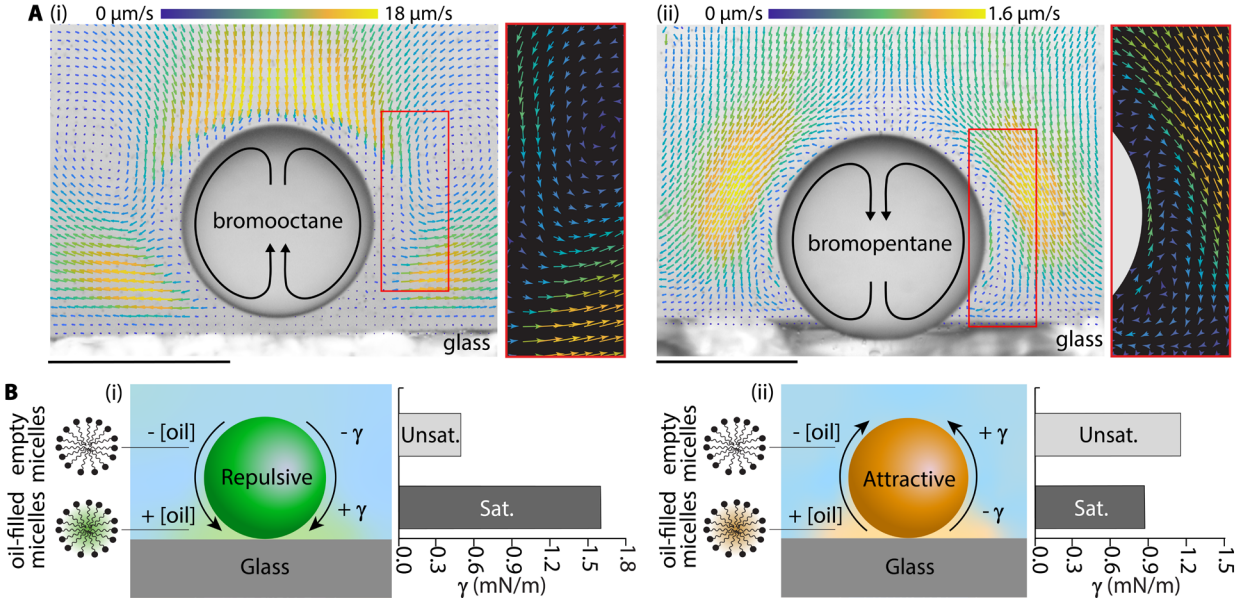

Figure 2: Attractive and repulsive drops differ in interfacial tension gradients and Marangoni flow. **A,** PIV mapping of Marangoni flows around isolated droplets of **(A-i)** repulsive bromooctane and **(A-ii)** attractive bromopentane in 2 wt% NP-12. The droplets sit on the bottom of a glass cuvette and are imaged through the cuvette side with an optical microscope (**Figure S1**). Overlaid arrows indicate the direction of particle motion and the arrow color indicates speed according to the color scale. Enlarged areas boxed in red highlight differing directions of flow near the side of the

droplet; the background image in the inset was removed to clearly see the arrow direction. **A-i,** Repulsive flows move down and away from the droplet interface. **A-ii,** Attractive flows move up the side of the droplet interface. Scale, 100 μm. **B,** Schematics and interfacial tensions (γ) of (**B-i**) repulsive bromooctane and (**B-ii**) attractive bromopentane in 2 wt% NP-12. Bar graphs show the γ of each oil in 2 wt% NP-12 with no oil saturation (unsat., i.e. empty micelles) and oil saturation of the aqueous phase (sat., i.e. oil-filled micelles). Schematics show the flow direction around the droplets and illustrate the corresponding concentration gradients of oil, ([oil]), and γ. **B-i,** For repulsive bromooctane, higher concentrations of oil near the bottom of the drop correspond to a higher interfacial tension (+γ) and lower concentrations of oil near the top correspond to lower interfacial tension (-γ). **B-ii,** For attractive bromopentane, higher concentrations of oil near the bottom of the drop correspond (-γ) and low concentrations of oil near the top of the droplet correspond to (+γ).

To quantify the influence of oil-filled vs. empty micelles on the interfacial tension along the drop surface, we used the pendant drop method to measure the interfacial tension, γ. (Refer to SI section "Interfacial tension measurements" and **Figure S2**). We measured γ for each oil in 2 wt% NP-12 that was either unsaturated or oil-saturated (i.e. had oil-filled micelles) (**Figure 2B**). For repulsive bromooctane, bromooctane-saturation of the surfactant caused higher γ compared to unsaturated surfactant (γ_{sat}=1.61 ± 0.03 mN/m, γ_{unsat} = 0.49 ± 0.04 mN/m) (**Figure 2B-i**). Attractive bromopentane displayed the opposite trend, where bromopentane-saturation led to a lower interfacial tension (γ_{sat}=0.87 ± 0.05 mN/m, γ_{unsat} = 1.16 ± 0.03 mN/m) (**Figure 2B-ii**). Hence, solubilized bromooctane in 2 wt% NP-12 increased the interfacial tension and acts as a chemorepellent, while solubilized bromopentane decreased the interfacial tension and acts as a chemoattractant.

Considering how oil saturation affected the interfacial tension for attractive and repulsive drops, together with the observed Marangoni flow direction along the interface which proceeds from low to high interfacial tension, these results suggest that there is a higher concentration of oil-filled micelles at the bottom of the droplets nearest the substrate. This result is reasonable to expect because the wall acts to block diffusion of solubilized oil. Since the oils are denser than water, we considered whether solutal buoyancy contributes to the formation of the gradients; experiments with oil plugs that touch the top and bottom wall of a capillary suggested that the wall was the more important factor. (Refer to SI section, "Consideration of solutal buoyancy effects"). The polarization in the concentration of oil-filled micelles leads to the vertical "pumping" flow and sometimes droplet levitation, even for droplets that are not laterally self-propelled. Such results are consistent with simulations of flow for low Péclet number droplets near a wall[16] and have also been observed previously[10-11].

Based on the data in **Figures 1,2** it appeared that several variables, including the droplet composition and surfactant conditions, were influential in determining whether droplets exhibited either repulsive or attractive flow. To gain insight into the balance of these governing chemical factors, we systematically investigated the flow behavior of a range of oils with varying carbon numbers (*n*= 5 to 16) in Tergitol NP-X surfactant, where X= 9, 12, 15, or 30 and represents the average number of ethylene oxide (EO) repeat units in the surfactant headgroup. Iodohexadecane was used as *n*=16 because bromohexadecane is less dense than water which presented experimental difficulty. We also tested surfactant concentrations between 1 wt% and 5 wt%, which are all orders of magnitude above the CMC of each surfactant (CMC = 0.006 wt%, 0.0085 wt%, 0.009 wt%, and 0.0157 wt% for NP-9, NP-12, NP-15, and NP-30, respectively, as reported by the supplier). We note that NP-9 has a very similar chemical structure to Triton X-

100, which is another nonionic surfactant previously used to generate active behavior in solubilizing droplets[8a, 10, 12]. For each combination of oil, surfactant type, and surfactant concentration, we produced droplets by vortex mixing and then introduced a single droplet (diameter 100-150 µm) to a cuvette containing surfactant solution and tracer particles. We waited 5 minutes for the drop to settle and for flows to stabilize, and then we observed the tracer particle flow around the droplet. Similar to **Figure 2**, we characterized the flow around each droplet as "repulsive", "attractive", or "inactive" (i.e. no directional Marangoni flow observable) based on the direction that tracer particles traveled (**Figure 3A**). The flow directions reported in **Figure 3A** were persistent, and we watched selected droplets for over 4 hours and the flow patterns did not change.

The data in **Figure 3A** reveal several trends, as highlighted in **Figure 3B**. For a given surfactant type and concentration, repulsive flows were favored for oils with higher carbon number, *n*, (lower water solubility) while attractive flows were favored for lower *n* (higher water solubility). For instance, in 3 wt% NP-12, *n*=5, 6 were attractive, while *n*=8-16 were repulsive. For a given oil and surfactant concentration, there was a tendency for the flows to transition from repulsive to attractive to inactive as the EO number of the surfactant increased. Bromooctane, for instance, was repulsive in 1 wt% NP-9 and NP-12, attractive in 1 wt% NP-15, and was inactive in 1 wt% NP-30. We found that solubilization rate decreased as EO number increased, with solubilization of bromooctane in NP-15 and NP-30 being an order of magnitude slower than in NP-9 and NP-12 (**Table S1**). In many cases, increasing the surfactant concentration for a given oil and surfactant type favored a transition from attractive to repulsive flows, especially for surfactants with lower EO numbers (X=9,12,15). For example, bromohexane in 1 to 3 wt% NP-12 was attractive and in 5 wt% was repulsive, a trend which was also reported in the multibody interactions in **Figure 1A**. Bromononane shows a similar switch in behavior when changing from 1 wt% to >2 wt% NP-15. We found this flow-direction reversal as a function of surfactant concentration surprising. We used the pendant drop method to measure γ of bromononane in oil-saturated (γ_{sat}) and unsaturated (γ_{unsat}) NP-15. In 1 wt% NP-15, $\gamma_{unsat} > \gamma_{sat}$ with 3.79±0.03 mN/m and 3.04±0.06 mN/m, respectively. In 3 wt% NP-15, $\gamma_{unsat} < \gamma_{sat}$ with 2.93±0.03 mN/m and 3.28±0.07 mN/m, respectively, which is consistent with a change in the flow direction. The same generalized trends as a function of surfactant concentration and oil carbon number also held for Makon TD-12 surfactant, which has the same average EO number as Tergitol NP-12 but has a tridecyl group as the hydrophobic tail.

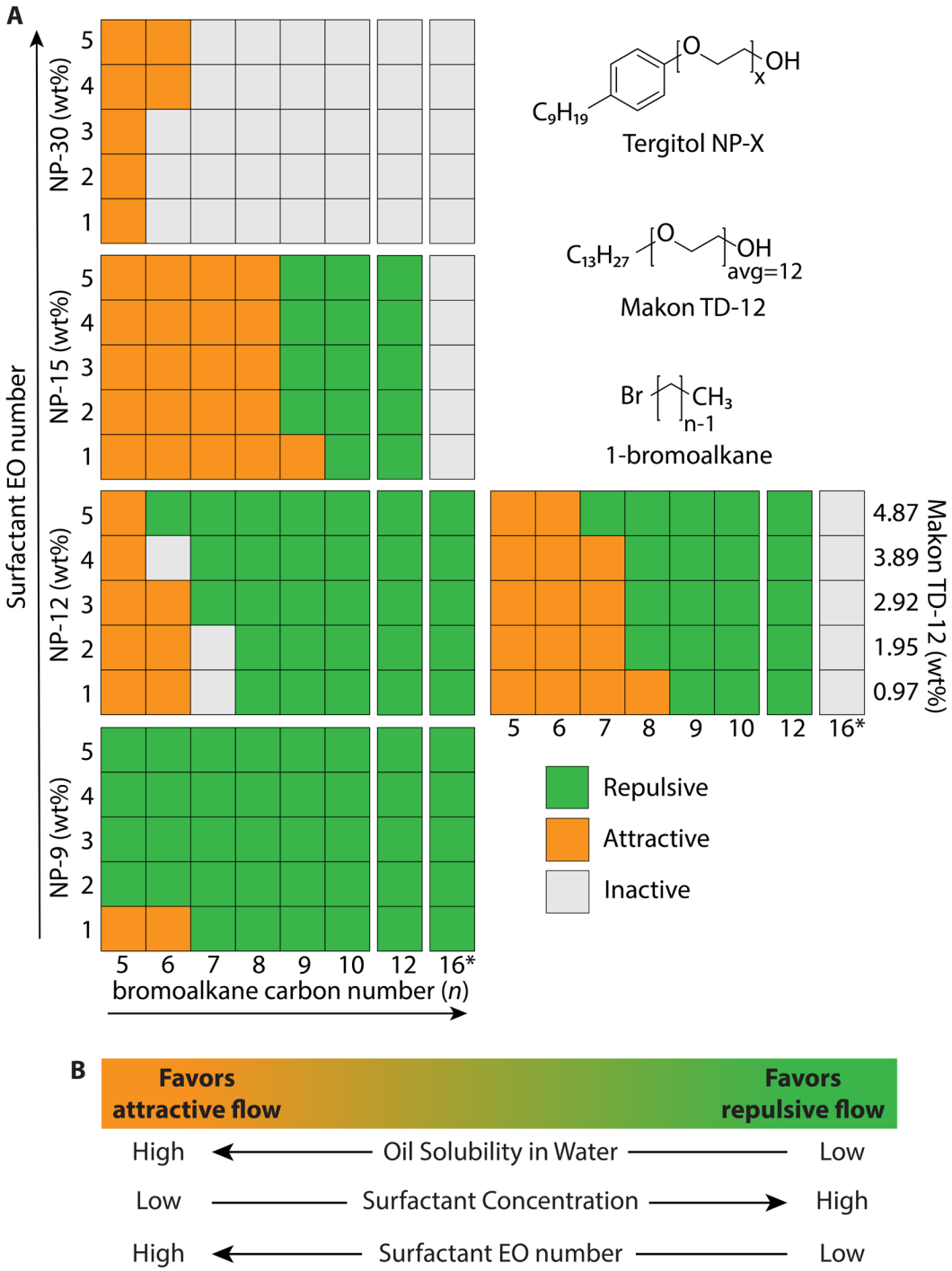

Figure 3: Oil carbon number, surfactant EO number, and surfactant concentration influence whether a droplet displays flows that are attractive, repulsive, or inactive. **A,** We analyzed the Marangoni flow around isolated oil droplets in aqueous surfactant for: varying haloalkane carbon number *n* (*n*= 5 to 16), varying Tergitol surfactant ethylene oxide (EO) number *X*, where *X*= 9, 12, 15, and 30 and is the average number of EO repeats, and varying surfactant concentrations (1 to 5 wt%). Bromoalkanes were used except for *n*=16*, where iodohexadecane was used because it sinks. A single droplet for each condition was analyzed as shown in **Figure 2**. Droplets were allowed to settle and equilibrate for 5 minutes, and then flow behavior was determined as indicated by the colored boxes: green is repulsive, orange is attractive, and grey indicates inactive (no observable directional flow). See **Table S1-S2** for solubilization rates. Makon TD-12 surfactant, which has the same average EO number as Tergitol NP-12 but has

a tridecyl group as the hydrophobic tail, was also investigated in equal molar concentrations to Tergitol NP-12 for comparison. **B,** From data in **A**, we observe trends: repulsive flows are favored for oils with low water solubility (higher *n*), higher surfactant concentrations, and surfactants with smaller headgroups (i.e. lower EO number). Attractive flows are favored for oils with higher water solubility (lower *n*), lower surfactant concentrations, and surfactants with larger headgroups (i.e. higher EO number).

We observed in **Figure 3A** conditions of inactivity falling between the attractive and repulsive flow regimes (e.g. bromohexane in 4 wt% NP-12). We investigated γ of bromohexane in oil-saturated (γ_{sat}) and unsaturated (γ_{unsat}) 4 wt% NP-12 and found γ_{unsat}= γ_{sat} = 1.04±0.07 mN/m. Curious as to how solubilization rates trend in the regions of inactivity, we measured the solubilization rates of bromohexane in 3 wt% and 4 wt% NP-12 which were 1.9±0.1 μm/min and 4.8±0.5 μm/min, respectively, and can be compared to the rates in 1 wt% and 5 wt% NP-12 reported earlier. Thus, bromohexane in 4 wt% NP-12 was still solubilizing at an appreciable rate, even though there was no observable connective flow. There were also many conditions of inactivity in **Figure 3A** for droplets in NP-30. We found that NP-30 is ineffective at micellar solubilization of most oils (**Table S1**) and only the more water-soluble oils (bromopentane and bromohexane) exhibited flow in NP-30. Iodohexadecane[10] also did not readily solubilize (**Table S2**) and hence was also more likely to exhibit inactivity due to negligible solubilization rate. Thus, while solubilization does not guarantee generation of Marangoni flow, solubilization is still a pre-requisite.

While **Figure 3** shows trends in the directionality of the flow (attractive vs repulsive), these classifications were not always related to flow speed. We define the flow speed as that of the fastest moving particles that were measurable near the droplet surface. For repulsive drops, the fastest flows were at the top of the droplet, and for attractive drops, flows were fastest along the sides. In most cases, repulsive flows were faster than attractive flows, as exemplified by the traces in **Figure 2A**, but this was not always the case. For repulsive iodohexadecane in 2 wt% NP-12, which solubilizes so slowly that a change in drop diameter was immeasurable over a 30-minute period (**Table S2**), the fastest tracer particles only moved at an average of 0.5 μm/s. Bromopentane in the same surfactant, which solubilizes readily, was attractive and tracer particles moved at an average of 1.6 μm/s. Again, we believe that the solubilization rate, which we report for a representative range of conditions in **Table S1-S2**, had an influence on the flow speed in combination with the other chemical factors.

The trends in **Figure 3** provide some chemical insights into tuning the flow direction using different combinations of oil and surfactant for situations wherein the droplet is solubilizing into the micelles. But what happens when the micelles are pre-filled with an oil that is different from the droplet oil? We examined the behavior of iodohexadecane drops in 3 wt% NP-12 pre-saturated with two different oils, bromopentane (chemoattractant, **Figure 4A-i**) or bromodecane (chemorepellent, **Figure 4A-ii**). We chose iodohexadecane as the droplet because it solubilizes very slowly as previously discussed and we were aiming to isolate the influence of the oil that was pre-filled in the micelles (**Figure 4B**). When placed in bromopentane or bromodecane-saturated surfactant, the iodohexadecane droplet diameter increased over time (**Figure 4B, Video S3**) indicating that the oil from the pre-filled micelles was transferring into the droplet faster than iodohexadecane was leaving. In bromopentane-saturated 3 wt% NP-12, the iodohexadecane drop still exhibited repulsive flow, as it had in the unsaturated surfactant (**Figure 4B-i**), but flow speeds were faster (3.8 μm/s vs. 0.5 μm/s). In bromodecane-saturated surfactant,

the iodohexadecane drop switched flow direction and was attractive (**Figure 4B-ii**). These same observations regarding droplet growth and flow directions held even when we replaced iodohexadecane with 1-(ethoxy)nonafluorobutane, an oil which has with no measurable solubilization or activity in 3 wt% NP-12 but is miscible with bromopentane and bromodecane. We propose that in all these cases, gradients of oil filled micelles (and hence variations in γ) are generated by oil transfer *into* the droplet, combined with symmetry breaking from the substrate. Through this chemical ripening process, micellar solution nearest the substrate is *depleted* of oil (**Figure 4B-i,ii**). Hence, the flow directions of the iodohexadecane or 1-(ethoxy)nonafluorobutane drop are consistent with expectations of the interfacial tension gradients created by concentration gradients of either the chemorepellent oil (bromodecane) or chemoattractant oil (bromopentane) (**Figure 4B**).

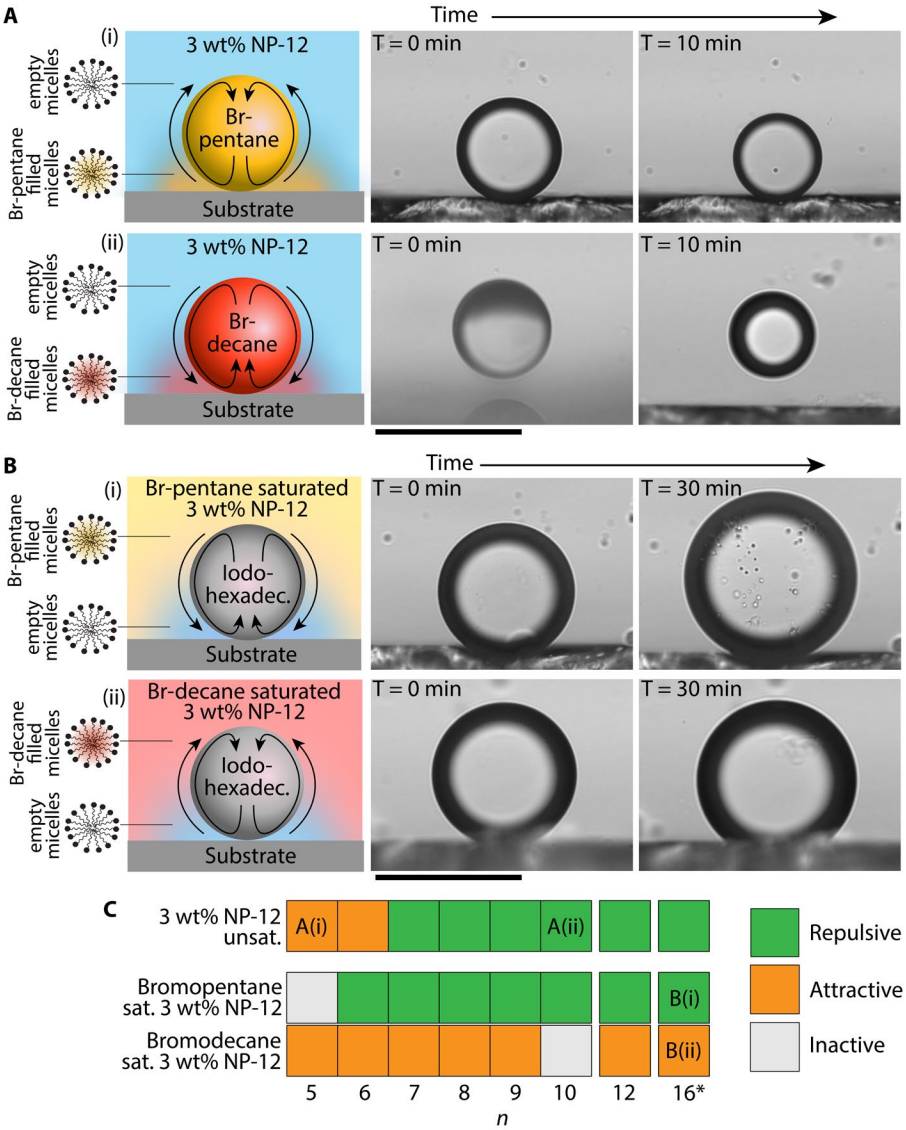

Figure 4: Modulating droplet behavior through saturation of the continuous phase with different oils. **A,** Left column: schematics of solubilizing **(A-i)** attractive bromopentane and **(A-ii)** repulsive bromodecane in unsaturated 3 wt% NP-12. Oil-filled micelle concentration is higher near the substrate as depicted by the gradient coloration.

Middle and right columns: timelapse optical micrographs of isolated bromopentane and bromodecane droplets solubilizing over time in unsaturated 3 wt% Tergitol NP-12. **B,** Left column: schematics of iodohexadecane drops in **(B-i)** bromopentane-saturated and **(B-ii)** bromodecane-saturated micellar solutions of 3 wt% NP-12. Iodohexadecane uptakes oil from the micelles, resulting in lower concentrations of oil-filled micelles near the substrate as depicted with the gradient coloration. Arrows around the droplet indicate flow direction, where **B-i** is repulsive and **B-ii** is attractive. Middle and right columns: timelapse optical micrographs of iodohexadecane droplets in the different oil-saturated surfactant solutions. The iodohexadecane droplet grows in diameter over time. **C**, Observed Marangoni flow behavior of isolated oil drops composed of bromoalkanes with carbon numbers *n*= 5 to 12 and iodohexadecane (n=16*) in unsaturated, bromopentane-saturated, and bromodecane-saturated 3 wt% NP-12. Data was collected in the same manner as for **Figure 3** and characterized as attractive (orange), repulsive (green), or inactive (grey). Scale 100 μm.

We next wanted to test how this chemical ripening process would affect the flow directions for droplets of oils which *do* solubilize. We analyzed the flow direction of droplets containing oils varying in carbon number (*n*=5 to 12) in bromopentane- or bromodecane-saturated 3 wt% NP-12 (**Figure 4C**). Most of the droplet flows in unsaturated surfactant were already repulsive, so the bromopentane-saturation had minor impact, only changing the flow of bromohexane from attractive to repulsive. Bromodecane-saturation, however, had a significant effect, causing all the droplets to exhibit attractive flow. A switch in flow direction between unsaturated and bromodecane-saturated surfactant suggests that into-drop transfer of bromodecane dominated the interfacial tension gradients and flow, overshadowing effects of out-of-drop solubilization. Whenever the droplet oil had a higher carbon number than the oil pre-filled into micelles, the droplet grew in diameter. Whenever the droplet had a lower carbon number oil than the oil pre-filled into micelles, the droplet still shrank, albeit more slowly than in unsaturated surfactant, and developed small droplets/aggregates near the drop interface, potentially from a supersaturation of oil leading to spontaneous emulsification[17] (**Video S4**). A more extensive dataset conducted with NP-9 for various oil-saturation conditions is given in **Figure S3**. In general, we find these results of **Figure 4** and **Figure S3** notable, because they indicate that Marangoni flows around active drops can be caused by oil transfer into, as well as out of, the droplet. Flow can be imparted to an otherwise non-solubilizing, inactive drop by introduction of a different oil into the continuous phase that partitions into the drop.

In current work studying active solubilizing droplets, higher concentrations of solubilizate have been correlated to higher interfacial tensions[1a], thereby acting as a chemorepellent which enables the feedback mechanism responsible for droplet self-propulsion[7, 14] as well as multibody droplet repulsion[11] and droplet chasing[12]. Here, we have described some contrary conditions wherein solubilized oil leads to decreased interfacial tension at oil-water interfaces, acting as a chemoattractant, and inducing attractive interactions between droplets. These “attractive-type” droplets are not laterally self-propelled, as would be expected, but they do exhibit vertical pumping flows due to symmetry breaking from the substrate. Whether a droplet is repulsive or attractive is influenced by the combination of all three variables considered: oil, surfactant, and surfactant concentration. The precise mechanism by which solubilization and the “filling” of micelles imparts changes to the droplet interfacial tensions under varying chemical conditions is still unclear, but our results suggest that the chemical effects are perhaps more nuanced than previously acknowledged. We consider here whether our results can provide insight as to why some oils, surfactants, and surfactant concentrations yield these different behaviors.

It is well known that addition of cosolvents to surfactants can change the CMC, so one possible explanation we considered for the variation in interfacial tensions between attractive and repulsive systems was that the surfactant CMC was being altered as a result of the oil micellar solubilization. For instance, it has been reported that diethyl phthalate oil decreases the CMC of sodium dodecyl sulfate (SDS), which could explain why diethyl phthalate droplets in SDS are self-propelled and repulsive[7]. Perhaps, attractive flows are a result of an increased CMC upon filling the micelles with certain oils. However, we observed in several instances that the flow direction changed between attractive and repulsive as a function of surfactant concentration. It does not seem likely to us that the CMC would increase, then decrease, as the surfactant concentration changes. Thus, while it cannot be ruled out entirely, a change in the CMC does not seem like a complete explanation for all observed droplet behaviors.

Another possibility is that the aggregation number of the surfactant (N) is different when the micelle is empty (N_e) compared to when the micelle is filled with oil (N_f). For conditions wherein droplets are self-propelled, it has been proposed[14] that $N_f > N_e$ such that there is a depletion of surfactant monomer in the vicinity of the drop surface, leading to an increase in interfacial tension. For attractive systems where solubilizate decreases interfacial tension, perhaps $N_f < N_e$. We used dynamic light scattering to measure the micelle size for a range of NP-12 and NP-15 concentrations with and without a few different solubilized oils (**Table S3**) that exhibit a range of attractive, repulsive, and inactive flow. Micelles with solubilized oil always had a larger hydrodynamic diameter than the micelles without oil and we did not find any correlation between micelle size and the interfacial tensions or flow directions. Admittedly, because oil molecules can also contribute to an increased micelle size, it is still possible that $N_f < N_e$ in some circumstances so these results were inconclusive.

Nonionic surfactants can partition from the aqueous phase into oil[18], so we considered whether surfactant accumulation in the droplet may be causing the different flow directions. Since ionic surfactants like sodium dodecyl sulfate (SDS) should not partition to a significant degree, we examined the flow directions around selected oils (bromopentane, bromooctane, and bromodecane) in 1, 3, and 5 wt% SDS (**Figure S4**). We still observed flow conditions that were attractive, repulsive, and inactive, suggesting that surfactant partitioning is not necessary. More extensive examination of the influence of ionic surfactants will be conducted in the future.

We focused our attention to the trends shown in **Figure 3.** Within the bounds of conditions tested in **Figure 3**, we found that attractive flow was favored by lower carbon number oils, larger surfactant EO numbers, and lower surfactant concentrations. Repulsive behavior was favored by higher carbon number oils, smaller surfactant EO numbers, and higher surfactant concentrations (**Figure 3B**). These trends interested us because they correlate with the two proposed mechanistic pathways by which oil can be transported across oil-water interfaces[19]: molecular transport and micellar transport (**Figure S5**). The contributions of these pathways to solubilization have been extensively discussed and debated in the literature[19-20]. We limit ourselves to primarily considering the interfacial processes in emulsions with nonionic surfactants only, because ionic surfactants would be reasonably expected to undergo somewhat different solubilization processes and transfer kinetics due to electrostatic repulsion between the droplet interface and the micelles[20g, 21]. For nonionic surfactants, both pathways are likely to simultaneously contribute to solubilization[20b] with the kinetic balance determined by the specific emulsion composition. In the molecular pathway, oil molecules diffuse into the

continuous aqueous phase before being incorporated into a micelle. In the micellar pathway, oil molecules are directly incorporated into micelles at the interface. It is reasonable to assume that micelles of nonionic surfactant can directly adsorb to the interface[22] rather than first dissociating into monomers. It is generally accepted that smaller, more water-soluble oils have a greater propensity to solubilize by the molecular pathway, while larger more hydrophobic oils are more likely to transfer via a micelle-mediated pathway[20b-d]. The pathway dependence of oil solubilization as a function of surfactant EO number is less well studied; it is speculated that higher EO numbers (i.e. larger surfactant headgroup sizes) lead to more steric repulsion between the micelle and drop interface which limits solubilization by micelles and would thus favor the molecular pathway[20g]. We anticipate that an increase in surfactant concentration above the CMC, which increases the concentration of micelles, would favor the micellar pathway.

Thus, we expect that a molecular pathway is favored for lower carbon number oils, larger surfactant EO numbers, and lower surfactant concentration, while a micellar pathway is favored for higher carbon number oils, smaller surfactant EO numbers, and higher surfactant concentrations. Interestingly, we find that the factors favoring the molecular pathway are also those associated with attractive droplet behavior and the factors favoring the micellar pathway are associated with repulsive droplet behavior. These results might suggest that, perhaps, a kinetic balance between transport pathways impacts the molecular structure and interfacial tension of droplet interfaces stabilized by nonionic surfactants while undergoing solubilization.

Conclusions

We systematically investigated the influence of oil chemical structure, nonionic surfactant structure, and surfactant concentration on the Marangoni flow behaviors of solubilizing oil-in-water droplets. We identified three “regimes”, designated as attractive, repulsive, or inactive, depending on the directionality of flow surrounding isolated solubilizing droplets sitting on a substrate. Droplet inactivity, wherein no convective flow is observed, can still occur even when the droplet is solubilizing at an appreciable rate. We demonstrated that transport of oil from pre-filled micelles into droplets, in addition to oil transfer out of the droplet into micelles, can also cause Marangoni flow. We observed correlations between oil chemical structure, nonionic surfactant chemical structure, and surfactant concentration and whether flow was attractive or repulsive. We suggest these relationships might hint at interfacial tensions being influenced by a kinetic balance of interfacial transport pathways. While our results are not conclusive in this regard, we think it is worth considering in future work how interfacial transport pathways play a mechanistic role. Potentially, competing effects (wherein some processes raise interfacial tension and some lower it) might be at play, which could be interesting for designing chemical feedback mechanisms in active emulsions. We hope these results will provide insight into how chemical parameters can be used to manipulate the dynamics and interactions in emulsions and contribute to building a foundation for design of more complex active and chemotactic materials.

Acknowledgments

We acknowledge support from the Charles E. Kaufman Foundation (1031373-438639), the AAAS through the Marion Milligan Mason Award (236764) and the Army Research Office (W911NF-18-1-0414).

Data availability statement. The data that support the findings of this study are available in the supplementary material of this article.

References

[1] a) C. C. Maass, C. Krüger, S. Herminghaus, C. Bahr, *Annu. Rev. Conden. Ma. P.* **2016**, *7*, 171-193; b) A. Zöttl, H. Stark, *J. Phys. Condens. Matter* **2016**, *28*, 253001; c) T. Liebchen, H. Löwen, *Acc. Chem. Res.* **2018**, *51*, 2982−2990; d) R. Seemann, J.-B. Fleury, C. C. Maass, *Eur. Phys. J.: Spec. Top.* **2016**, *225*, 2227-2240; e) D. Lohse, X. Zhang, *Nat. Phys. Rev.* **2020**, *2*, 426–443; f) J. Ignés-Mullol, F. Sagués, *Curr. Opin. Colloid. In.* **2020**, *49*, 16–26.

[2] Z. Izri, M. N. Van Der Linden, S. Michelin, O. Dauchot, *Phys. Rev. Lett.* **2014**, *113*, 248302.

[3] a) T. Banno, R. Kuroha, T. Toyota, *Langmuir* **2012**, *28*, 1190-1195; b) T. Ban, T. Yamagami, H. Nakata, Y. Okano, *Langmuir* **2013**, *29*, 2554-2561; c) M. M. Hanczyc, T. Toyota, T. Ikegami, N. Packard, T. Sugawara, *J. Am. Chem. Soc.* **2007**, *129*, 9386-9391; d) N. J. Suematsu, K. Saikusa, T. Nagata, S. Izumi, *Langmuir* **2019**, *35*, 11601–11607; e) S. Thutupalli, R. Seemann, S. Herminghaus, *New J. Phys.* **2011**, *13*, 073021; f) S. Thutupalli, S. Herminghaus, *Eur. Phys. J. E* **2013**, *36*, 91; g) T. Toyota, N. Maru, M. M. Hanczyc, T. Ikegami, T. Sugawara, *J. Am. Chem. Soc.* **2009**, *131*, 5012-5013; h) D. Babu, R. J. H. Scanes, R. Plamont, A. Ryabchun, F. Lancia, T. Kudernac, S. P. Fletcher, N. Katsonis, *Nat. Commun.* **2021**, *12*, 2959.

[4] a) Y. Xiao, S. Zarghami, K. Wagner, P. Wagner, K. C. Gordon, L. Florea, D. Diamond, D. L. Officer, *Adv. Mater.* **2018**, *30*, 1801821; b) S. Zhang, C. Contini, J. W. Hindley, G. Bolognesi, Y. Elani, O. Ces, *Nat. Commun.* **2021**, *12*, 1673; c) I. Lagzi, S. Soh, P. J. Wesson, K. P. Browne, B. A. Grzybowski, *J. Am. Chem. Soc.* **2010**, *132*, 1198-1199; d) M. Rajabi, H. Baza, H. Wang, O. D. Lavrentovich, *Front. Phys.* **2021**, 682.

[5] C. Jin, C. Krüger, C. C. Maass, *P. Natl. Acad. Sci. USA* **2017**, *114*, 5089-5094.

[6] S. Michelin, E. Lauga, D. Bartolo, *Phys. Fluids* **2013**, *25*, 061701.

[7] A. Izzet, P. G. Moerman, P. Gross, J. Groenewold, A. D. Hollingsworth, J. Bibette, J. Brujic, *Phys. Rev. X* **2020**, *10*, 021035.

[8] a) C. H. Meredith, A. Castonguay, Y.-J. Chiu, A. M. Brooks, P. G. Moerman, P. Torab, P. K. Wong, A. Sen, D. Velegol, L. D. Zarzar, *Matter* **2022**, *5*, 616-633; b) M. Li, M. Brinkmann, I. Pagonabarraga, R. Seemann, J.-B. Fleury, *Commun. Phys.* **2018**, *1*, 23; c) X. Wang, R. Zhang, A. Mozaffari, J. J. de Pablo, N. L. Abbott, *Soft Matter* **2021**, *17*, 2985-2993; d) M. Li, M. Hosseinzadeh, I. Pagonabarraga, R. Seemann, M. Brinkmann, J.-B. Fleury, *Soft Matter* **2020**, *16*, 6803-6811.

[9] N. Ueno, T. Banno, A. Asami, Y. Kazayama, Y. Morimoto, T. Osaki, S. Takeuchi, H. Kitahata, T. Toyota, *Langmuir* **2017**, *33*, 5393-5397.

[10] S. I. Cheon, L. Batista Capaverde Silva, A. Khair, L. Zarzar, *Soft Matter* **2021**, *17*, 6742-6750.

[11] P. G. Moerman, H. W. Moyses, E. B. Van Der Wee, D. G. Grier, A. Van Blaaderen, W. K. Kegel, J. Groenewold, J. Brujic, *Phys. Rev. E* **2017**, *96*, 032607.

[12] C. H. Meredith, P. G. Moerman, J. Groenewold, Y.-J. Chiu, W. K. Kegel, A. van Blaaderen, L. D. Zarzar, *Nat. Chem.* **2020**, *12*, 1136-1142.

[13] a) C. Krüger, C. Bahr, S. Herminghaus, C. C. Maass, *Eur. Phys. J. E* **2016**, *39*, 64; b) S. Thutupalli, J.-B. Fleury, U. D. Schiller, G. Gompper, S. Herminghaus, R. Seemann, in

Engineering of Chemical Complexity II, Vol. 12, World Sci. Singapore, **2014**, p. 125; c) B. Kichatov, A. Korshunov, V. Sudakov, V. Gubernov, A. Golubkov, A. Kiverin, *Langmuir* **2021**, *37*, 9892–9900; d) C. Jin, Y. Chen, C. C. Maass, A. J. Mathijssen, *Phys. Rev. Lett.* **2021**, *127*, 088006.

[14] S. Herminghaus, C. C. Maass, C. Krüger, S. Thutupalli, L. Goehring, C. Bahr, *Soft Matter* **2014**, *10*, 7008-7022.

[15] M. Morozov, *Soft Matter* **2020**, 5624--5632.

[16] N. Desai, S. Michelin, *arXiv preprint arXiv:2111.01437* **2021**.

[17] C. A. Miller, *Colloid Surface* **1988**, *29*, 89-102.

[18] F. Ravera, M. Ferrari, L. Liggieri, *Advances in colloid and interface science* **2000**, *88*, 129-177.

[19] S. R. Dungan, B. H. Tai, N. I. Gerhardt, *Colloid Surf. A* **2003**, *216*, 149-166.

[20] a) P. Neogi, *J. Colloid Interf. Sci.* **2003**, *261*, 542-546; b) S. Ariyaprakai, S. R. Dungan, *Langmuir* **2008**, *24*, 3061-3069; c) B. J. Carroll, *J. Colloid Interf. Sci.* **1981**, *79*, 126-135; d) A. J. Ward, in *P. Roy. Irish. Acad. B*, JSTOR, **1989**, pp. 375-382; e) A. C. Donegan, A. J. Ward, *J. Pharm. Pharmacol.* **1987**, *39*, 45-47; f) D. J. Luning Prak, L. M. Abriola, W. J. Weber, K. A. Bocskay, K. D. Pennell, *Environ. Sci. Technol.* **2000**, *34*, 476-482; g) A. A. Peña, C. A. Miller, *Adv. Colloid Interface Sci.* **2006**, *123*, 241-257.

[21] a) P. D. Todorov, P. A. Kralchevsky, N. D. Denkov, G. Broze, A. Mehreteab, *J. Colloid Interf. Sci.* **2002**, *245*, 371-382; b) A. S. Kabalnov, *Langmuir* **1994**, *10*, 680-684.

[22] D. M. Colegate, C. D. Bain, *Phys. Rev. Lett.* **2005**, *95*, 198302.

Table of Contents

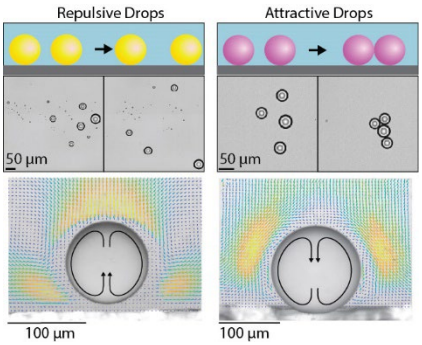

We systematically characterize the influence of oil chemical structure, nonionic surfactant structure, and surfactant concentration on the interfacial tensions and Marangoni flows of solubilizing oil-in-water drops. Three regimes corresponding to droplet “attraction”, “repulsion”, or “inactivity” are identified and the chemical trends leading to these behaviors are discussed.

Key words: active matter, emulsions, micelles, solubilization, surfactants, interfaces

Supporting information for:

Chemically tuning attractive and repulsive interactions between solubilizing oil droplets

Ciera M. Wentworth[1], Alexander C. Castonguay[1], Pepijn G. Moerman[2], Caleb H. Meredith[3], Rebecca V. Balaj[1], Seong Ik Cheon[1], Lauren D. Zarzar[1,3,4]

1. Department of Chemistry, The Pennsylvania State University, University Park, PA 16802, USA
2. Department of Chemical and Biomolecular Engineering, Johns Hopkins University, Baltimore, MD 21218, USA
3. Department of Materials Science and Engineering, The Pennsylvania State University, University Park, PA 16802, USA
4. Materials Research Institute, The Pennsylvania State University, University Park, PA 16802, USA

This document contains

1. Detailed experimental methods
2. Tables S1-S3
3. Figures S1-S5
4. Captions for Video S1-S4
5. References

Experimental Section

Chemicals
All chemicals were used as received. 1-bromopentane (99%) (Alfa Aesar); 1-bromohexane (99%) (Alfa Aesar); 1-bromoheptane (>98%) (Toyoko Chemical Industry); 1-bromooctane (>98%) (Toyoko Chemical Industry); 1-bromononane (99%) (Alfa Aesar); 1-bromodecane (>98%) (Toyoko Chemical Industry); 1-bromododecane (>98%) (Alfa Aesar); 1-iodohexadecane (>98%, stabilized with copper) (Alfa Aesar); Tergitol NP-9 (Sigma); Tergitol NP-12 (The Dow Chemical Company); Tergitol NP-15 (The Dow Chemical Company); Tergitol NP-30 (The Dow Chemical Company); Makon TD-12 (Stepan Company); polybead carboxylate 1.0 micron microspheres (Polysciences Inc.); 1-(ethoxy)nonafluorobutane, mixture of n- and iso-butyl (Synquest); sodium dodecyl sulfate (Sigma-Aldrich); *N*-(triethoxysilylpropyl)-o-polyethylene oxide urethane (95%) (Gelest); hexadecyltrimethoxysilane (>85%) (Sigma-Aldrich).

Emulsion preparation
Polydisperse droplets were produced by adding ~50 µL of oil and ~300 µL of surfactant solution to a glass vial and vortex mixed.

Substrate preparation
Unless otherwise noted, all substrates were untreated glass. If the glass was functionalized, the following procedure was used. Glass coverslips were thoroughly washed with acetone, a reagent alcohol solution (largely ethanol), and water, then treated with base bath for one hour (2 M potassium hydroxide). After drying, the coverslips were surface functionalized with one of two silanes to generate either hydrophilic or hydrophobic glass. For hydrophilic surface treatment, coverslips were placed in in 100 mL of 0.3 v/v% *N*-(triethoxysilylpropyl)-o-polyethylene oxide urethane in toluene solution overnight. For hydrophobic surface treatment, coverslips were placed overnight in 100 mL of 1.0 v/v% hexadecyltrimethoxysilane in hexane. Finally, the coverslips were rinsed with toluene and ethanol and dried in the oven at 50 °C overnight.

Preparation of oil-saturated surfactant solutions
Oil-saturated surfactant solutions were prepared by adding 400-600 µL of bromoalkane oil to 20 mL of aqueous Tergitol surfactant (1 to 5 wt%, in NP-9, NP-12, NP-15, and NP-30) and placed on a tube rotator for at least four days, and sometimes longer times were needed. We observed that shorter bromoalkanes took both more oil and longer times to reach saturation. Saturation was tested by observing the flow around a droplet of the same oil used to saturate the solution; the solution was deemed saturated if no observable flow was present. Approximate oil solubilities, in µL oil per mL solution, were found for select oil-surfactant systems by incrementally adding a few microliters of oil at a time to the surfactant solution and waiting for the oil to disappear before adding more. These experiments were conducted to elucidate trends in the relative solubility of different carbon number oils in surfactants of different EO number and surfactant concentration. Higher carbon number oils have reduced solubility, higher concentrations of surfactant lead to higher solubility, and higher EO number surfactants cause reduced solubility. Results are included below. We also note that the oil solubilization capacity of the micellar solutions is much larger than the volumes of the oil droplets used in the experiments (about $5x10^{-4}$ µL) such that the volume ratio of the water to oil phase is not a limiting factor in the solubilization of droplets.

	1 wt% NP-9	1 wt% NP-12	1 wt% NP-15	5 wt% NP-12
Bromohexane	~ 9 µL/mL	~ 5 µL/mL	< 3 µL/mL	>17 µL/mL
Bromodecane		< 2.5 µL/mL		

Multi-droplet behavior observations and optical microscopy
Droplet behaviors and interactions were observed by using an inverted optical microscope (Nikon, Eclipse Ti-U) in brightfield transmission mode between 4x and 20x magnification and images were recorded with an Andor Zyla 4.2P sCMOS camera. Droplets were prepared by vortex mixing (see above for emulsion preparation) and ~40 droplets were added via pipette to a 1.5” diameter coverslip-bottom dish containing ~ 1 mL of the same surfactant solution in which the droplets were prepared.

Side-orientation flow visualization and optical microscopy
Visualization of the vertical flows around the haloalkane droplets was conducted using a custom-built transmission microscope comprised of a white LED for illumination, a microscope objective (10x, Nikon), and a 200 mm tube lens (Thorlabs) coupled to a CMOS camera (Basler). The light and objective lens were oriented parallel to the sample substrate to enable visualization of the droplet profile as it sits on the substrate. To prepare the continuous phase, 1 drop of tracer particles (1 μm, Polysciences Inc.) was added to 10 mL of desired surfactant solution to make a tracer stock. 400 μL of this tracer particle/surfactant solution was added to a thin (~3 mm width) glass cuvette. Droplets of haloalkane (see above for emulsion preparation) were first dispersed into a dish and a single droplet was extracted via pipette and placed into the cuvette. After adding the single oil droplet to the tracer particle/surfactant solution in the cuvette, the droplet was moved to one side of the cuvette for better image contrast and allowed to sit for 5 minutes to reduce the influence of external flow in the container.

Particle tracking for flow maps and speed measurements
Flow maps for select oil systems were created using videos gathered from the side-orientation flow visualization experiments with tracer particles (see above). Data analysis was conducted using a combination of customized MATLAB code and PIVlab, a particle image velocimetry code available for MATLAB.[1-3] Flow maps were made by averaging the frame-to-frame flow vectors generated in PIVlab using our custom code on unaltered data from PIVlab analysis. Reported flow speeds were then gathered from these averaged profiles where we were able to clearly visualize the fastest particle flow, which was at a distance of ~30 microns from the droplet surface for attractive flow conditions or ~10 microns away from the top of the droplet for repulsive flow conditions. Flows that were closer to the droplet interface may be faster than those reported but were difficult to measure accurately by PIV.

Solubilization rate measurements
The droplet diameter was recorded as a function of time to extract a solubilization rate. Solubilization rates reported in the main text were collected by extracting and isolating a single droplet (starting diameter of approximately 200 microns) with a pipette from a coverslip-bottom dish containing ~100 polydisperse droplets (see above for emulsion preparation), transferring the single droplet into a coverslip-bottom dish containing surfactant (~ 1 mL), placing a coverslip on top to reduce convection, and tracking drop diameter over time. Solubilization rates reported in **Table S1** and **Table S2** were collected similarly except that a concave-depression glass slide covered with a cover glass was used to confine the droplet, which reduced overall droplet motion and had a lower volume of continuous phase surfactant solution (0.3 mL). We found that solubilization rates tended to be slower in the concave-depression slide, but more consistent between repeated trials. In all cases, droplets were viewed on a Nikon Eclipse Ts2 using an Imaging Source DFK 23UX249 color camera between 4x-20x magnification. Images were taken every 15 minutes using IC Capture 2.4 software. Droplet diameter was tracked for at least a 30-minute period. Droplet diameters were measured using the diameter function in Image J and plotted to obtain a fitted linear slope value, -dD/dt, which we define as the solubilization rate. The average of three trials was reported and the uncertainty is the standard deviation of the three trials. Over the diameter range of droplets used, spanning approximately 200 μm to 50 μm, the drop diameter decreases linearly with time; this allowed us to define the solubilization rate using the slope from a linear fit of drop diameter vs time data. Within this diameter range, the solubilization rate does not depend on the initial drop diameter.

Interfacial tension measurements
The pendant drop method on a Ramé-hart 250-U1-R automatic goniometer was used to measure the interfacial tension of bromoalkane-water systems. For “unsaturated” samples, pure bromoalkane was dispensed from a 22-gauge stainless steel needle into aqueous Tergitol surfactant solution within a glass cuvette. For “oil-saturated” samples, oil-saturated surfactant solutions were used as the continuous phase. Oil-saturated surfactant solution was prepared as described above in the section “Preparation of oil-saturated surfactant solutions”. For both unsaturated and saturated systems, the Drop Image Advanced software was used to obtain 200 interfacial tension measurements with a three second interval between measurements with drop volume control used to ensure a consistent drop volume. The last 30 measurements were averaged to obtain an interfacial tension value and each system was run in triplicate. After the 6-minute measurement period, some droplets, especially those in unsaturated surfactant, still had

interfacial tensions that were trending down very slowly but had largely stabilized (**Figure S2**). Saturated surfactant solutions reached a stable interfacial tension value within this 6-minute timeframe.

Micelle size measurements

Average micelle hydrodynamic diameter was measured using dynamic light scattering analysis on a Malvern Zetasizer. 1 mL of surfactant solution was placed in a quartz cuvette and allowed to equilibrate for 10 seconds before measurements were performed. All measurements were run in triplicate.

Consideration of solutal buoyancy effects

All the oils and the surfactants used in our experiments are denser than water. We considered whether solutal buoyancy was playing a role in generating the gradients around the droplets and the relative influence of buoyancy compared to the wall hindering diffusion and flow. We conducted an experiment with 2 wt% Tergitol NP-12 inside a rectangular glass capillary (1 mm wide, 0.1 mm thick). The oil plug touched both the top and bottom walls of the glass capillary, which we imaged from the side to determine tracer particle flow around the plug profile (see diagram below). If solutal buoyancy was important in causing the buildup of oil-filled micelles near the wall, then we would expect to see a different flow profile around the oil plug at the top wall compared to the bottom wall. However, we found repulsive flows at the top and bottom walls that were of similar flow speeds. This experiment suggests that effects of solutal buoyancy are small.

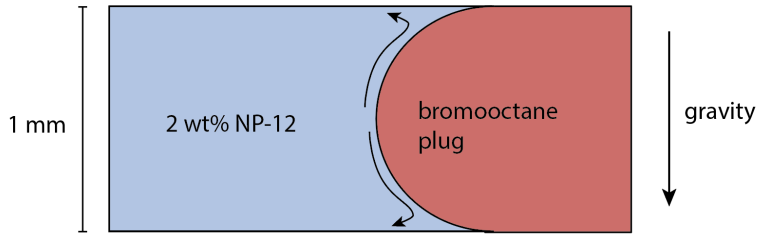

Table S1. Comparison of solubilization rates (-dD/dt) of bromooctane drops in Tergitol surfactants of varying EO length. Surfactants are named "NP-X" where "X" is the average number of ethylene oxide (EO) repeat units in the surfactant headgroup. Larger EO groups led to slower solubilization rate. Solubilization rates were determined by tracking the diameter of a single droplet as it solubilizes in a concave-depression glass slide over a 30-minute period with a coverslip top. The average of three trials was reported and the uncertainty is the standard deviation of the three trials. If we could not measure a change in the droplet size within the resolution of the optical microscope, we considered this solubilization to be "negligible".

Surfactant	Concentration (wt%)	Droplet oil	Solubilization rate (μm/min)
Tergitol NP-9	2	1-Bromooctane	3.97 ± 0.05
Tergitol NP-12			2.82 ± 0.14
Tergitol NP-15			0.29 ± 0.03
Tergitol NP-30			negligible

Table S2 Comparison of solubilization rates (-dD/dt) of oils with varying carbon number in Tergitol NP-12. Solubilization rates were taken by measuring the diameter a single droplet over time as it solubilizes in a concave-depression glass slide with a coverslip on top to minimize evaporation over a 30 to 75-minute period. The average of three trials was reported and the uncertainty is the standard deviation of the three trials. 0.005 wt% is below the CMC and all other concentrations are above the CMC. Bromopentane dissolved in 0.005 wt% at a rate almost as high as in 2 wt% surfactant, suggesting that, due to high water solubility, bromopentane dissolves primarily by water dissolution instead of micellar solubilization. Bromooctane did not dissolve in 0.005 wt% but readily solubilized in 2 wt%, indicating solubilization by a micelle-mediated pathway. Intermediate carbon number oils solubilized the fastest in 2 wt% and very long chain oils (e.g. iodohexadecane) solubilized to a minimal extent. If we could not measure a change in the droplet size within the resolution of the optical microscope, we considered this solubilization to be "negligible".

Surfactant	Concentration (wt%)	Droplet oil	Solubilization rate (μm/min)
Tergitol NP-12	0.005	1-Bromopentane	0.36 ± 0.07
		1-Bromooctane	negligible
Tergitol NP-12	2	1-Bromopentane	1.25 ± 0.08
		1-Bromooctane	2.82 ± 0.14
		1-Bromodecane	1.16 ± 0.15
		1- Iodohexadecane	negligible

Table S3. Micelle size in various Tergitol surfactant solutions with and without oil saturation. The hydrodynamic diameter of the micelle was measured by dynamic light scattering. Average micelle size calculated from three trials. Reported uncertainty is the standard deviation of those three trials. All oil saturated samples also contained a peak in 200-400 nm range which is assumed to be mesoscale structures, perhaps similar to those reported in the literature for other binary and ternary mixtures[4-5].

Surfactant	Concentration (wt%)	Oil saturated	Hydrodynamic Diameter of Micelle (nm)
Tergitol NP-12	1	None	7.8 ± 0.1
		1-Bromohexane	12.4 ± 0.1
	3	None	7.3 ± 0.1
		1-Bromohexane	12.0 ± 0.1
		1-Bromodecane	9.4 ± 0.2
	5	None	7.0 ± 0.1
		1-Bromohexane	11.7 ± 0.2
Tergitol NP-15	1	None	7.5 ± 0.1
		1-Bromononane	8.7 ± 0.1
	3	None	7.0 ± 0.1
		1-Bromohexane	9.0 ± 0.3
		1-Bromononane	8.0 ± 0.1
		1-Bromodecane	8.1 ± 0.1

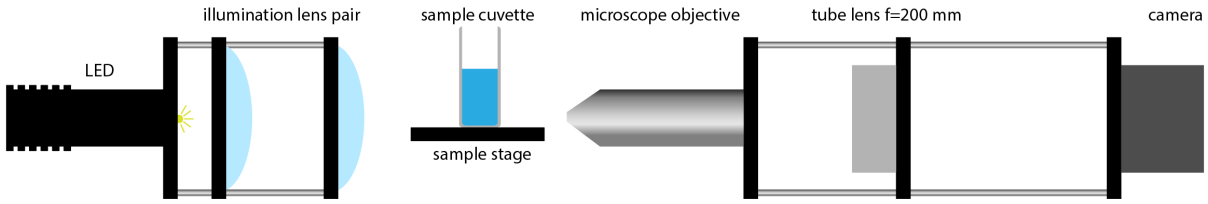

Figure S1. Schematic of the microscope setup used to visualize droplets sitting on the bottom of a cuvette substrate by looking through the side of the cuvette.

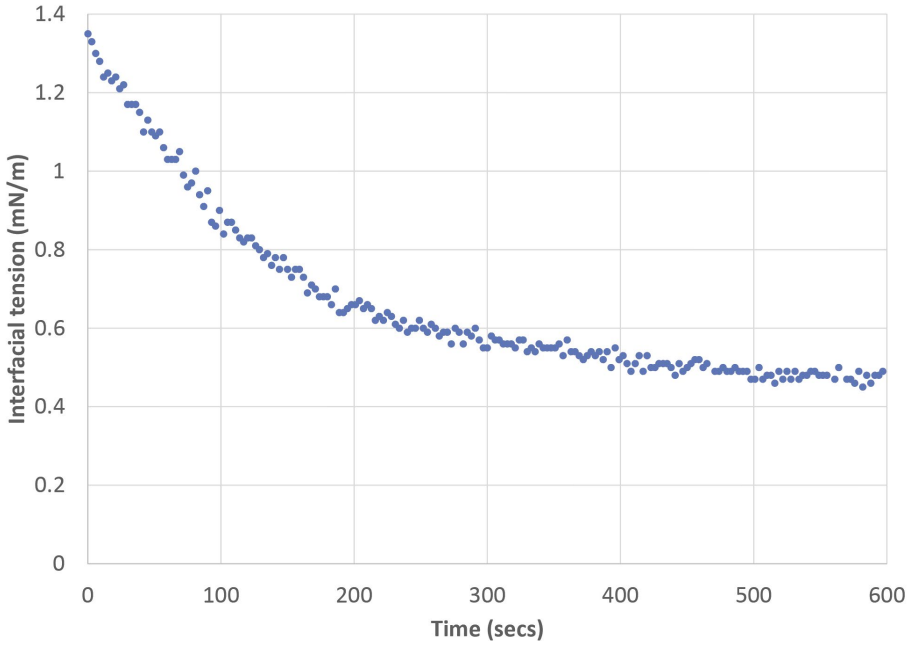

Figure S2. Dynamic interfacial tension for bromooctane in 2 wt% Tergitol NP-12.

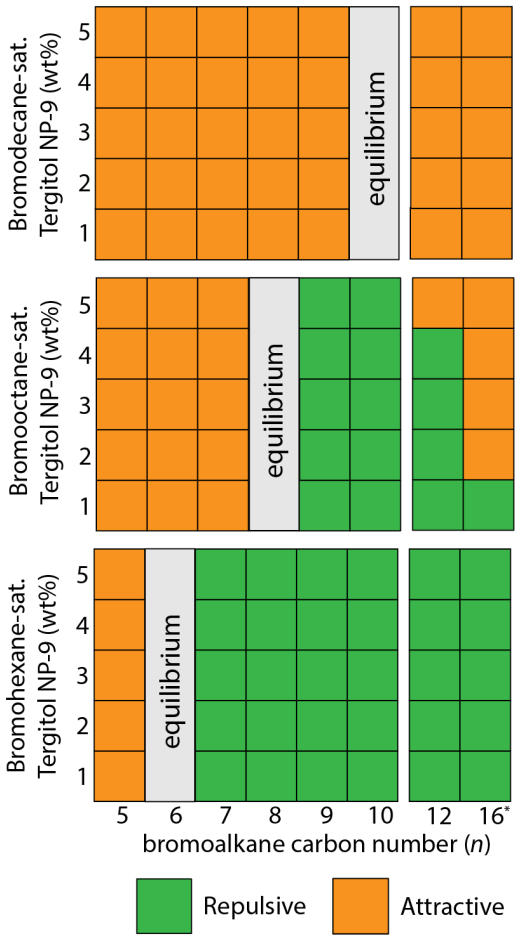

Figure S3. Pre-saturation of Tergitol NP-9 with different oils significantly affects the flow behavior of droplets. The Marangoni flow around isolated droplets of bromoalkane carbon number (n=5 to 12) and iodohexadecane* were examined in bromohexane-, bromooctane-, and bromodecane-saturated 1 to 5 wt% Tergitol NP-9. This data is directly comparable to **Figure 3** which depicts flows for the unsaturated surfactant condition**.** All droplets with a lower carbon number than the saturating oil shrank over time and developed a "halo" of a different refractive index material around the droplet edge, similarly to shown in **Video S4**; potentially, it is an excess of solubilized oil. Droplets with a higher carbon number than the saturating oil grew in diameter over time suggesting that there was a net transfer of oil into the droplet.

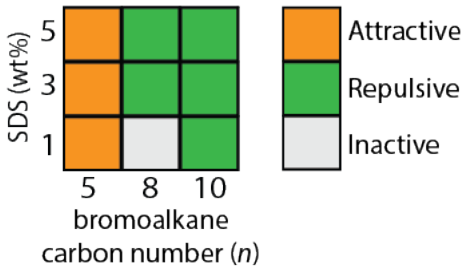

Figure S4. Flows of selected bromoalkanes in ionic surfactant sodium dodecyl sulfate (SDS). The Marangoni flows around isolated droplets of bromopentane, bromooctane, and bromodecane in 1, 3, and 5 wt% SDS were examined as outlined in experimental section “Side-orientation flow visualization and optical microscopy”.

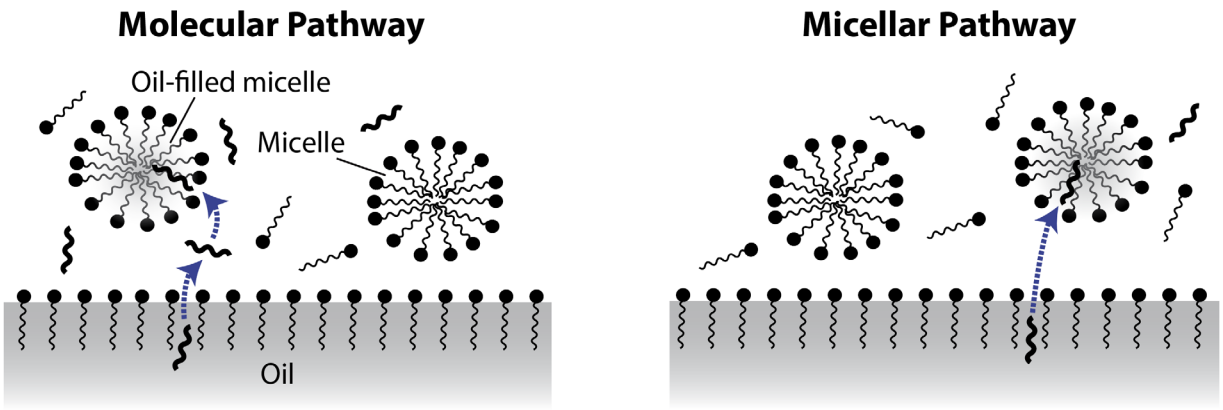

Figure S5. Oil solubilization pathways. Oil is proposed to solubilize via two pathways, the molecular pathway and the micellar pathway. In the molecular pathway, oil molecules diffuse into the continuous aqueous phase before being incorporated into a micelle. In the micellar pathway, oil molecules are directly incorporated into micelles at the interface.

Supporting video captions

Video S1. Solution flow around a bromooctane drop in 2 wt% Tergitol NP-12. 1 μm polystyrene tracer particles were used to visualize the flow surrounding a droplet of bromooctane dispersed in a 2 wt% Tergitol NP-12. These particles move from the top of the droplet, down the sides, then pump away from the bottom of the droplet. We note that bromooctane can be self-propelled at this concentration of Tergitol NP-12, but here we find that the droplet is levitating without lateral motion. This flow is representative of "repulsive flow" and PIV maps are given in **Figure 2Ai**. Scale 50 μm. Real time.

Video S2. Solution flow around a bromopentane drop in 2 wt% Tergitol NP-12. 1 μm polystyrene tracer particles were used to visualize the flow surrounding a droplet of bromopentane dispersed in a 2 wt% Tergitol NP-12. The particles are drawn towards the bottom of the droplet near the substrate and flow part way up the droplet side. This flow pattern is representative of "attractive flow" and PIV maps are given in **Figure 2Aii**. Scale 50 μm. 5x speed.

Video S3. An iodohexadecane drop in a bromopentane-saturated solution of 3 wt% Tergitol NP-12 grows in diameter over time. The iodohexadecane droplet increases in diameter over time when placed in 3 wt% Tergitol NP-12 solution saturated with bromopentane, indicating a net inward flux of bromopentane oil into the droplet. Scale 50 μm. 300x speed.

Video S4. A bromopentane droplet shrinks in a bromooctane-saturated solution of 3 wt% Tergitol NP-12. Droplets that are composed of a shorter carbon chain length oil than is saturated in the surfactant shrink and develop a halo-like area of small aggregates / droplets near the droplet interface. Scale 50 μm. 10x speed.

References

1. Meredith, C. H.; Castonguay, A.; Chiu, Y.-J.; Brooks, A. M.; Moerman, P. G.; Torab, P.; Wong, P. K.; Sen, A.; Velegol, D.; Zarzar, L. D., Chemical design of self-propelled Janus droplets. *Matter* **2022,** *5* (2), 616-633.
2. Thielicke, W.; Stamhuis, E. J., PIVlab-time-resolved digital particle image velocimetry tool for MATLAB. *Published under the BSD license, programmed with MATLAB* **2014,** *7* (0.246), R14.
3. Thielicke, W.; Stamhuis, E., PIVlab–towards user-friendly, affordable and accurate digital particle image velocimetry in MATLAB. *Journal of open research software* **2014,** *2* (1).
4. Zhang, Y.; Chen, X.; Liu, X., Temperature-induced reversible-phase transition in a surfactant-free microemulsion. *Langmuir* **2019,** *35* (44), 14358-14363.
5. Sedlák, M.; Rak, D., Large-scale inhomogeneities in solutions of low molar mass compounds and mixtures of liquids: supramolecular structures or nanobubbles? *The Journal of Physical Chemistry B* **2013,** *117* (8), 2495-2504.